

Tensorial Constitutive Models for Disordered Foams, Dense Emulsions, and other Soft Nonergodic Materials

M. E. Cates

School of Physics, University of Edinburgh,
JCMB, King's Buildings,
Mayfield Road, Edinburgh, EH9 3JZ, UK.

P. Sollich

Department of Mathematics, King's College,
University of London, Strand, London, WC2R 2LS, UK.

2 May 2003

Abstract

In recent years, the paradigm of ‘soft glassy matter’ has been used to describe diverse nonergodic materials exhibiting strong local disorder and slow mesoscopic rearrangement. As so far formulated, however, the resulting ‘soft glassy rheology’ (SGR) model treats the shear stress in isolation, effectively ‘scalarizing’ the stress and strain rate tensors. Here we offer generalizations of the SGR model that combine its nontrivial aging and yield properties with a tensorial structure that can be specifically adapted, for example, to the description of fluid film assemblies or disordered foams.

1 Introduction

Many soft materials, including foams, dense emulsions, slurries, pastes, and textured morphologies of liquid crystals, are characterized by the presence of structural disorder on a mesoscopic scale (nanometres to microns), causing metastability and slow dynamical evolution. Such materials are nonergodic, and can therefore be viewed, in at least one sense, as glasses. In the current work we address only shear-thinning materials (for generalizations to shear thickening see Head et al. (2001, 2002)) where data for the steady state flow curve are very often fitted either to (a) the ‘Herschel-Bulkley’ form, $\sigma(\dot{\gamma}) - \sigma_Y \sim \dot{\gamma}^p$, where $\sigma_Y > 0$ is a yield stress and $0 < p < 1$; or (b) to the ‘power law fluid’ form which is the same except with $\sigma_Y = 0$. (A survey of edible soft matter (Holdsworth, 1993) lists a very large number of instances of such fits in the literature.) The linear rheological spectra are also often close to power law fluid form, or else exhibit near constant storage modulus $G'(\omega)$ and anomalously flat or even rising loss modulus $G''(\omega)$ as frequency is decreased. In many instances, aging effects are seen (Höhler et al., 1999; Cloître et al., 2000; Cohen-Addad and Höhler, 2001; Viasnoff and Lequeux, 2002; Viasnoff et al., 2003; Cloître et al., 2003) in which the material gradually gets more elastic and less lossy as time goes by. These

effects can be quite complicated, with the rate of aging depending on stress (Cloître et al., 2000).

2 The SGR Model

Much of the aforementioned phenomenology, including some but not all aspects of the observed aging behavior, are captured by a simple and generic model called the SGR (or ‘soft glassy rheology’) model (Sollich et al., 1997; Sollich, 1998; Fielding et al., 2000). This model is based on Bouchaud’s trap model of glasses (Bouchaud, 1992; Bouchaud et al., 1995), and envisages mesoscopic elements whose dynamics consists of independent hopping between local traps (or free energy minima). In the context of e.g. a foam, such ‘hopping’ events correspond to yielding, where a cluster of bubbles rearranges into a new and more energetically favourable topological structure. The hopping is controlled by an effective temperature parameter $x = T_{\text{eff}}/T_g$ which lies near a glass transition ($x \simeq 1$). Such a transition exists if, as we shall assume, the distribution of trap depths is exponential. This choice allows many-body effects (which are undoubtedly present near any glass transition) to be ignored without losing the transition altogether, and is therefore an intrinsic part of the trap model picture as usually formulated.

In its original form (Sollich et al., 1997; Sollich, 1998) which addresses only simple shear flows, the SGR model combines the hopping dynamics of Bouchaud’s model with the buildup of local elastic shear strains in the mesoscopic elements; these are assumed, between hops, to be linearly elastic and to deform affinely with the applied flow. Upon hopping, the local strain l is reset to zero. The stored elastic energy density $kl^2/2$ (with k an elastic modulus) in each element is offset against the trap depth and lowers the local activation barrier to hopping; this leads to shear thinning. The dynamics of the SGR model is contained in the time evolution equation for the probability distribution $P(E, l, t)$ for a mesoscopic element being in a trap of depth E (> 0) with local shear strain l :

$$\dot{P}(E, l, t) = -\dot{\gamma} \partial P / \partial l - \Gamma_0 e^{-(E - kl^2/2)/x} P(E, l, t) + \Gamma(t) \rho(E) \delta(l) \quad (1)$$

Here Γ_0 is an intrinsic jump rate, and $\Gamma(t) = \int \Gamma_0 e^{-(E - kl^2/2)/x} P(E, l, t) dE dl$ is the overall jump rate allowing for the modulation of barriers by the strain; $\rho(E) = \exp(-E)$ denotes the distribution of trap depths into which elements can jump. Note that in proper dimensional units, we should write $(E - v kl^2/2)/(x k_B T_g)$ instead of $(E - kl^2/2)/x$, with v the volume of an element. In the following, we choose to measure energy densities such as $kl^2/2$ in units of $k_B T_g/v$, and energies such as E in units of $k_B T_g$, so that the extra dimensional factors disappear. The macroscopic shear stress is taken to obey

$$\sigma(t) = \int P(E, l, t) kl dE dl. \quad (2)$$

For a detailed discussion of how the aforementioned flow and aging phenomenology arises from this SGR model, see Sollich et al. (1997); Sollich (1998); Fielding et al. (2000). A review which puts this in a broader context is Cates

(2003). There are, of course, many open issues with the model. One of these concerns the interpretation of the noise temperature x and whether or not this should depend on flow history: in this paper we assume it does not. Also, the rheological aging predictions of the model, though surprisingly rich (Fielding et al., 2000; Viasnoff and Lequeux, 2002; Viasnoff et al., 2003), do not include all those found experimentally; see e.g. Höhler et al. (1999); Cloître et al. (2000); Cohen-Addad and Höhler (2001). Nonetheless, the model represents a useful step towards understanding the rheology of materials that are not time-translation invariant (Fielding et al., 2000).

A separate shortcoming of the SGR model lies in its tensorial simplicity. Because simple shear flow and linear local elasticity are both assumed, no normal stresses can ever arise. The strain variable l in Eq.1 is effectively a scalar, as is the macroscopic shear stress σ . The form chosen for the shear thinning is also quite restricted. In what follows we address these shortcomings by showing how the SGR model can be ‘tensorialized’ with minimal damage to the appealing phenomenology that it contains. This allows for various forms of nonlinear elasticity at the mesoscale, and also lets us consider arbitrary deformation histories rather than just simple shear.

Our starting point is the constitutive equation for the standard, scalar SGR model, whose derivation (Sollich, 1998) we briefly recall here. We imagine that at the zero of time the sample is prepared in a known state that has, for simplicity, all mesoscopic elements unstrained; this assumption could be relaxed, but saves algebra. This state is characterized by $P(E, l, 0) = P_0(E)\delta(l)$. The constitutive equation then reads

$$\sigma(t) = G_0(z_{t0})k\gamma(t) + \int_0^t \Gamma(t')G_1(z_{tt'})k[\gamma(t) - \gamma(t')]dt' \quad (3)$$

Here $G_0(z_{t0})$ is the fraction of elements present originally (at $t = 0$) surviving to time $t > 0$. The factor $k\gamma(t)$ is the stress they contribute. The integral is over elements created at $t' < t$, with creation rate $\Gamma(t')$ and survival probability $G_1(z_{tt'})$ to time t ; each has been strained through $\gamma(t) - \gamma(t')$ and contributes stress accordingly. The following equations complete the prescription (Sollich, 1998):

$$1 = G_0(z_{t0}) + \int_0^t \Gamma(t')G_1(z_{tt'})dt' \quad (4)$$

$$z_{tt'} = \int_{t'}^t \exp\left(k[\gamma(t'') - \gamma(t')]^2/2x\right)dt'' \quad (5)$$

$$G_0(z) = \langle e^{-z\Gamma_0 \exp(-E/x)} \rangle_{P_0} \quad ; \quad G_1(z) = \langle e^{-z\Gamma_0 \exp(-E/x)} \rangle_\rho \quad (6)$$

Equation 4 fixes, by normalization, the jump rate $\Gamma(t')$ required in Eq.3. Equation 5 defines an ‘effective time interval’ z between times t and t' ; this is defined in such a way as to absorb the factor by which the jump rate out of a trap is enhanced due to the presence of a strain. In other words, within the scalar SGR model, the nonlinear effect of shear can be viewed as ‘making the clock tick faster’ for any element that has accumulated nonzero value of the local strain l since its creation. Indeed, this is the *only* nonlinearity in the model, which is why Eq.6

defines the survival functions for each class of element exactly as one would in Bouchaud’s model, except that z replaces t .

3 Tensorial SGR Models

We now turn to the main agenda, which is to relax the tensorially naive assumptions of the SGR model as formulated thus far. Fortunately the structure and interpretation of the scalarized SGR constitutive equation, Eq.3, allow one very easily to construct various tensorial descriptions based on the same underlying physics, but with more specific and fully tensorial models for the local elastic and yield behaviour of the mesoscopic elements. Because the connection with Bouchaud’s trap model remains intact, these models will retain the interesting aging behavior and spectral phenomenology outlined in the introduction. The same applies to flow curves although these will be somewhat modified by any additional nonlinearities now introduced at the mesoscale.

We present this first for a schematic dumbbell based SGR model. A somewhat simpler class of models, closer in spirit to the scalar SGR picture, is then suggested. Members of this class adapted to describe the case of foams and dense emulsions, are then studied in more detail.

3.1 A Dumbell SGR Model

We consider an ensemble of dumbbell-like objects. Each dumbbell is characterized by an end-to-end vector $\mathbf{u} \equiv u_\mu$ of length $u \equiv |\mathbf{u}|$; the stress contributed by such dumbbells is deemed to be $\sigma_{\mu\nu} = nk\langle u_\mu u_\nu \rangle_P$ where the average is over a distribution function $P(E, \mathbf{u}, t)$; n is the density of dumbbells and k an elastic constant. (The units of k are, in this section, different from those used previously; e.g. $ku^2/2$ has the dimensions of an energy and is therefore assumed to be expressed in dimensionless multiples of $k_B T_g$.) Thus far, apart from the appearance of the E variable, this formulation resembles a first step towards the upper convected Maxwell model (Cates, 2003), where the dumbbell dynamics consists of two particles advected by the flow connected by a spring. (This is often used as a model for sub-entangled polymers.) In the present context we are not restricted to thinking of our dumbbells as polymers; they represent unspecified elastic objects, each of which is held in place by its neighbors but can make discrete stochastic rearrangements that relax its stress locally.

SGR-like dynamics (quite unlike that of the Maxwell model) is now introduced by assuming that each dumbbell follows the flow affinely, except that from time to time it makes a jump to a completely new configuration, with a jump rate $\Gamma_0 \exp[-(E - ku^2/2)/x]$. Here E is an energy barrier which is lowered by the stored elastic energy $ku^2/2$. (One can imagine the dumbbells as hooked into a network of neighbors, which deforms affinely; but when a particular dumbbell becomes too elongated, its connections to the network will be more likely to break.) After a jump, the dumbbell is assigned a new yield energy E drawn from the usual prior distribution $\rho(E) = e^{-E}$. It is also assigned at random a new value of \mathbf{u} , drawn from the equilibrium distribution at noise temperature x , $p_{\text{eq}}(\mathbf{u}) \sim \exp(-k\mathbf{u}\cdot\mathbf{u}/2x)$.

The resulting equation of motion, closely analogous to Eq.1, is

$$\dot{P}(E, \mathbf{u}, t) = -(\partial P / \partial \mathbf{u}) \cdot \mathbf{K} \cdot \mathbf{u} - \Gamma_0 \exp[-(E - ku^2/2)/x] P + \Gamma(t) \rho(E) p_{\text{eq}}(\mathbf{u}) \quad (7)$$

with \mathbf{K} the rate-of-strain tensor and $\Gamma(t) = \Gamma_0 \langle \exp[-(E - ku^2/2)/x] \rangle_P$ the total jump rate. A new feature is the appearance of $p_{\text{eq}}(\mathbf{u})$ in the last term to replace $\delta(l)$ in the scalar SGR model: this is the closest we can get to the assumption, made there, of ‘zero strain’ in new mesoscopic elements without actually setting \mathbf{u} to zero (in which case every dumbell would collapse to a point and never be stretched under the affine flow). This choice will recover Boltzmann equilibrium for the \mathbf{u} (at temperature x) in the absence of flow, which is not true of the scalar model: but it is a moot point whether this *should* be recovered, since x is not a true temperature (Sollich et al., 1997; Sollich, 1998). An alternative choice, probably not much different in practice, would be to use $4\pi p_{\text{eq}}(\mathbf{u}) = \delta((\mathbf{u} \cdot \mathbf{u})^{1/2} - (3x/k)^{1/2})$, corresponding to the selection of new dumbells with random directions on a sphere of radius $\langle u^2 \rangle_{\text{eq}}^{1/2} = 3x/k$.

Now assume that at time zero a system is prepared by some definite process (e.g. a quench) that gives a known initial distribution of dumbell barrier heights and vectors $P(E, \mathbf{u}, 0) = P_0(E) p_0(\mathbf{u})$ (chosen factorable for simplicity). Then, following the same arguments as lead to Eq.3, the constitutive equation can be written (with an additional coefficient α discussed below)

$$\begin{aligned} \alpha^{-1} \sigma_{\mu\nu}(t) = & \langle G_0(z_{t0}(\mathbf{u})) n k(\mathbf{E}_{t0} \cdot \mathbf{u})_{\mu} (\mathbf{E}_{t0} \cdot \mathbf{u})_{\nu} \rangle_{p_0} \\ & + \int_0^t \Gamma(t') \langle G_1(z_{tt'}(\mathbf{u})) n k(\mathbf{E}_{tt'} \cdot \mathbf{u})_{\mu} (\mathbf{E}_{tt'} \cdot \mathbf{u})_{\nu} \rangle_{p_{\text{eq}}} dt' . \end{aligned} \quad (8)$$

Here $\mathbf{E}_{tt'}$ is the deformation tensor between times t' and t , while G_0, G_1 are precisely as defined in Eq.6; the total jump rate $\Gamma(t)$ is found from

$$1 = \langle G_0(z_{t0}(\mathbf{u})) \rangle_{p_0} + \int_0^{t'} \Gamma(t') \langle G_1(z_{tt'}(\mathbf{u})) \rangle_{p_{\text{eq}}} dt' \quad (9)$$

and the ‘effective time’ variable z , which is now explicitly dependent on the end-to-end vector \mathbf{u} with which an element was created, obeys

$$z_{tt'}(\mathbf{u}) = \int_{t'}^t \exp(k |\mathbf{E}_{t''t'} \cdot \mathbf{u}|^2 / 2x) dt'' . \quad (10)$$

The above constitutive equation involves, as well as a tensorial dependence on strain of the elastic stress and of the yield energy, an extra layer of averaging over the \mathbf{u}_i variables describing the end-to-end vectors with which dumbells were created after their most recent jump. This makes its quantitative analysis (which must mainly be done numerically from this point onwards) rather cumbersome and we do not pursue it in this paper. Nonetheless, it is clear by the construction of the model that its behavior in simple shear flows will differ relatively slightly from the scalar SGR model; we should expect Herschel-Bulkley ($x < 1$) and power-law-fluid ($x > 1$) flow curves with power law $G^*(\omega)$ spectra at $x > 1$ and aging behavior, very similar to that described by Fielding et al. (2000), for $x \leq 1$. But, unlike the scalar version, the model is capable of nontrivial predictions for

normal stresses under shear and also for the rheological and aging behavior in elongational and mixed flows.

The model just presented has some features in common with that of Michel et al. (2001). If the dumbbells are thought of as polymer strands, it could be used to represent physical gels with cross links having a broad (in the model, exponential) distribution of activation energies. As formulated so far, these energy barriers are lowered in height by the full stored energy in a network strand between links. This is surely an exaggeration, since in practice only a part of that energy can be converted into the work of breaking a link. However, to improve this correspondence one could choose $\alpha > 1$ in Eq.8. In this case the stored energy appearing in the lowering of energy barriers is only a fraction $1/\alpha$ of the elastic energy of the strand, whereas the full value is used to calculate the macroscopic state of stress. (Equivalently, the plateau modulus in the model is now larger by a factor of α .)

3.2 A Better Class of Model

The extra averaging required above, in passing from the scalar to the dumbbell SGR model, is rather a nuisance. Arguably, though, it ought to be redundant. After all, the basic elements of the SGR picture were not intended to represent individual polymers or particles (as the dumbbell idea tacitly assumes) but mesoscopic elements, within which a degree of local averaging can already be presumed. One could thus hope for a simpler description in which such elements have a distribution of yield energies E , but otherwise are taken as isotropic bodies with a well-behaved, deterministic elastic response, albeit in most cases nonlinear. No averaging over \mathbf{u}_i would be necessary if we replaced our dumbbells with elastic spheres, for example.

The general structure of the SGR-type constitutive equation that results from this assumption of local averaging within a meso-element is as follows:

$$\boldsymbol{\sigma}(t) = G_0(z_{t0})\mathbf{Q}(\mathbf{E}_{t0}) + \int_0^t \Gamma(t')G_1(z_{tt'})\mathbf{Q}(\mathbf{E}_{tt'}) dt' \quad (11)$$

$$z_{tt'} = \int_{t'}^t \exp [R(\mathbf{E}_{t''t'})/x] dt'' \quad (12)$$

with G_0, G_1 and $\Gamma(t)$ obeying Eqs.4,6. Here \mathbf{Q} and R are tensor and scalar functions of \mathbf{E} that can be freely chosen. Suitable choices for foams and dense emulsions are suggested below, but models for other specific materials could employ quite different forms for these. By construction, the pre-averaged tensorial models defined by Eqs.11,12 are, for bland choices of \mathbf{Q} and R , again expected to behave rather like the scalar SGR model (with glass transition at $x = 1$, aging and power-law fluid regimes etc.), while at the same time describing nontrivial normal stress effects under shear flow, and offering tractable models for the behavior of soft glassy materials in extensional flow. Shear thickening models, along the lines developed from the scalar SGR model by Head et al. (2001, 2002), could also be introduced with suitable choices of \mathbf{Q} and R ; in particular, if \mathbf{Q} is not strongly strain-thinning, a choice of R that drops sharply at intermediate strains

and rises again for large ones should lead to shear-thickening (and perhaps static jamming) behavior (Head et al., 2001, 2002).

3.3 Tensorial SGR Models for Foams and Dense Emulsions

Turning now to foams and dense emulsions, what are suitable choices for \mathbf{Q} and R ? The first of these determines (to within a factor of the plateau modulus G which we set equal to unity below) the stress created in a mesoscopic element as a result of a deformation. In particular, the instantaneous response to a nonlinear step strain is wholly controlled by \mathbf{Q} . Therefore it fixes, for example, the ratio $\varphi = N_2/N_1$ of first normal stress differences in such an instantaneous response. Another significant quantity, closely related to \mathbf{Q} , is the ratio $\chi = G/\mathcal{F}_0$ between the elastic modulus and the stored free energy density \mathcal{F}_0 , which resides in the interfacial energy of the fluid films in an unstrained state. On dimensional grounds, G and \mathcal{F} are proportional; each scales as σ/ξ where σ is an interfacial tension and ξ a characteristic length scale associated with a foam droplet.

Turning to the scalar quantity R , this represents the lowering of rearrangement barriers due to stored strain energy. In principle the lowering of a barrier could have a somewhat complicated dependence on the deformation \mathbf{E} of the given element, but we assume for simplicity that it depends only on the free energy density $\mathcal{F}(\mathbf{E})$ in a mesoscopic element under strain. Moreover, again for the sake of simplicity, we assume this dependence is linear:

$$R(\mathbf{E}) = \lambda \frac{\mathcal{F}(\mathbf{E}) - \mathcal{F}_0}{\mathcal{F}_0} \quad (13)$$

where λ is a parameter that should be, with our choice of units, of order one. (This parameter obviates the need for the parameter α introduced earlier in Eq.8; it plays the same role of determining what fraction of the stored elastic energy can be used as work to overcome a rearrangement barrier.) With R defined as in Eq.13, the ratio χ can be read off from an expansion for small shear strain γ as $R = \lambda\chi\gamma^2/2 + \dots$.

We now introduce three possible models for the elasticity of fluid film assemblies (foams and dense emulsions) that predict approximate forms for both the step-strain response tensor $\mathbf{Q}(\mathbf{E})$ and the stored free energy $\mathcal{F}(\mathbf{E})$ as a function of deformation. All expressions are given only for the relevant case of incompressible flows, $\det(\mathbf{E}) = 1$.

Model 1. This model is inspired by the work of Doi and Ohta (1991) who addressed the rheology of emulsion droplets under flow (albeit with no attempt to address the foam limit, where droplets are in close proximity). For simplicity, Doi and Ohta assumed affine deformation of an isotropic assembly of fluid interfaces. Their result for \mathbf{Q} may be written

$$Q_{\mu\nu}(\mathbf{E}) = -\frac{15}{4} \frac{1}{4\pi} \int \frac{u_\mu u_\nu - \frac{1}{3}\delta_{\mu\nu}}{|\mathbf{E}^T \cdot \mathbf{u}|^4} d^2u \quad (14)$$

where the integral is over the surface of a unit sphere; the corresponding form for R (using Eq.13) is

$$\frac{R(\mathbf{E})}{\lambda} = \frac{1}{4\pi} \int \frac{d^2u}{|\mathbf{E}^T \cdot \mathbf{u}|^4} - 1. \quad (15)$$

Model 1 has $\chi = 4/15$. For small shear strains one finds $Q_{xx} = (8/21)\gamma^2$, $Q_{yy} = -(13/21)\gamma^2$, $Q_{zz} = (5/21)\gamma^2$ and hence $\varphi = -7/6$, while for large strains $\varphi = -1$ as follows from $Q_{xx} = -Q_{yy}/2 = Q_{zz} = (5/8)\gamma$. For uniaxial *extension* both \mathbf{Q} and R can be found explicitly as shown by Doi and Ohta (1991); see Eqs.23,24 below.

Model 2. This is a restricted simplification of Model 1, again following Doi and Ohta (1991) who presented a tractable analytic approximant for \mathbf{Q} in the case of shear deformations only. In cartesian coordinates (x, y, z) with shear along x and gradient along y , the resulting \mathbf{Q} for shear strain γ is:

$$\mathbf{Q}(\gamma) = (1 + \gamma^2/3)^{-1/2} \begin{pmatrix} \gamma^2/3 & \gamma & 0 \\ \gamma & -2\gamma^2/3 & 0 \\ 0 & 0 & \gamma^2/3 \end{pmatrix} \quad (16)$$

and the expression for the effect of strain on stored energy, Eq.13, gives:

$$\frac{R(\gamma)}{\lambda} = (1 + \gamma^2/3)^{1/2} - 1. \quad (17)$$

Model 2 has $\varphi = -1$ at all strains and $\chi = 1/3$.

Model 3. This is based on the work of Larson (1997) who, unlike Doi and Ohta, was explicitly addressing the case of dense foams. He modelled the fact that, in such a foam, an affine deformation does not preserve the 120° contact angles between fluid films; it should therefore be followed by a very fast local relaxation which will not show up in rheology. Larson's model for the step strain tensor \mathbf{Q} reads

$$\mathbf{Q}(\mathbf{E}) = -2\mathbf{C}^{1/2} + \frac{2}{3}(\text{tr } \mathbf{C}^{1/2})\mathbf{1} \quad (18)$$

where \mathbf{C} is the Cauchy strain tensor, obeying $\mathbf{C}^{-1} = \mathbf{E}^T \mathbf{E}$, and $\mathbf{C}^{1/2}$ is the symmetric tensor with $\mathbf{C}^{1/2} \cdot \mathbf{C}^{1/2} = \mathbf{C}$. The resulting stored energy expression gives (via Eq.13):

$$\frac{R}{\lambda} = \frac{\text{tr } \mathbf{C}^{1/2}}{3} - 1. \quad (19)$$

Model 3 has $\varphi = -3/4$ at small strains and $\varphi \rightarrow -1$ at large ones; it predicts $\chi = 1/6$ (Larson, 1997). These are considerably closer to the values found numerically (Reinelt and Kraynik, 2000), at least for dry foams, than those for Models 1 and 2. This is hardly surprising since the Doi-Ohta analysis that underlies those models does not allow for the constancy of contact angles between films. (Nonetheless, for simplicity we stick to the latter for the numerics in the next section.)

We note in passing that Larson (1997) suggests a number of other general forms for the tensor \mathbf{Q} adapted, for example, to an assembly of elastic rather than fluid films; these could be chosen, within the tensorial SGR framework developed here, to address the flow of glassy assemblies of such objects.

3.4 Numerical Results

We now present a selection of numerical results, focussing on Model 1 and its close approximation for shear strain, Model 2. Throughout, we work in time units such that the microscopic time scale $\Gamma_0^{-1} = 1$.

The simplest case is a instantaneous step deformation \mathbf{E} . We assume that before this is applied the system is in equilibrium, which implies $x > 1$ since for smaller x the SGR model exhibits aging (Fielding et al., 2000). From Eq.11 one then deduces, by arguments exactly analogous to those of Sollich (1998), that the decay of the stress with time t after the step deformation is given by

$$\boldsymbol{\sigma}(t) = \mathbf{Q}(\mathbf{E})G_{\text{eq}}(t \exp[R(\mathbf{E})/x]) \quad (20)$$

Here the time-dependence is given by the same equilibrium stress relaxation function as in the scalar SGR model,

$$G_{\text{eq}}(z) = \frac{\int_z^\infty dz' G_1(z')}{\int_0^\infty dz' G_1(z')} \quad (21)$$

As in the scalar case, nonlinearities in the time-dependence arise only from the factor $\exp[R(\mathbf{E})/x]$, which produces a speed-up of the stress relaxation for large deformations. However, additional nonlinear effects occur in the tensorial model, through the instantaneous stress response $\mathbf{Q}(\mathbf{E})$. An interesting feature of Eq.20 is that all components of the stress tensor relax with the *same* time-dependence. This implies for example that the normal stress difference ratio $\varphi = N_2/N_1$ is independent of time, a prediction which could be tested experimentally.

In figure 1 we show example results for step shear, obtained from Model 2. These demonstrate the nonlinearities in both the instantaneous stress response and the time dependence of the subsequent stress relaxation. Only the results for σ_{xy} are shown; the relaxation curves for $N_1 = -N_2$ only differ through a constant factor which reflects their different initial values.

To emphasize that the tensorial SGR model can deal with deformations other than simple shear, we show in figure 2 analogous results for uniaxial extension, with deformation tensor

$$\mathbf{E} = \begin{pmatrix} e^{-\epsilon/2} & 0 & 0 \\ 0 & e^{-\epsilon/2} & 0 \\ 0 & 0 & e^\epsilon \end{pmatrix} \quad (22)$$

In this case we can use directly the unapproximated Model 1 since the integrals over \mathbf{u} in Eqs.14,15 can be performed analytically (Doi and Ohta, 1991). The stress tensor $\mathbf{Q}(\mathbf{E})$ is diagonal, with $Q_{xx} = Q_{yy} = -2Q_{zz}$ and¹

$$Q_{zz} = \frac{5}{8(e^{3\epsilon} - 1)} \left[e^{2\epsilon} + 2e^{-\epsilon} + (e^{5\epsilon} - 4e^{2\epsilon}) \tau(e^{3\epsilon} - 1) \right], \quad \tau(a) \equiv \frac{\arctan \sqrt{a}}{\sqrt{a}} \quad (23)$$

while the effect of deformation on stored energy is given by

$$\frac{R}{\lambda} = \frac{1}{2} \left[e^{-\epsilon} + e^{2\epsilon} \tau(e^{3\epsilon} - 1) \right] - 1 \quad (24)$$

¹In Doi and Ohta (1991), the prefactor $(e^{3\epsilon} - 1)^{-1}$ appears to have been omitted from the second term in the square brackets of Eq.23, presumably due to a typographical error. For $\epsilon < 0$ and hence $a < 0$, the function $\tau(\cdot)$ is defined by its natural analytic continuation, $\tau(a) = \text{artanh}(\sqrt{-a})/\sqrt{-a}$.

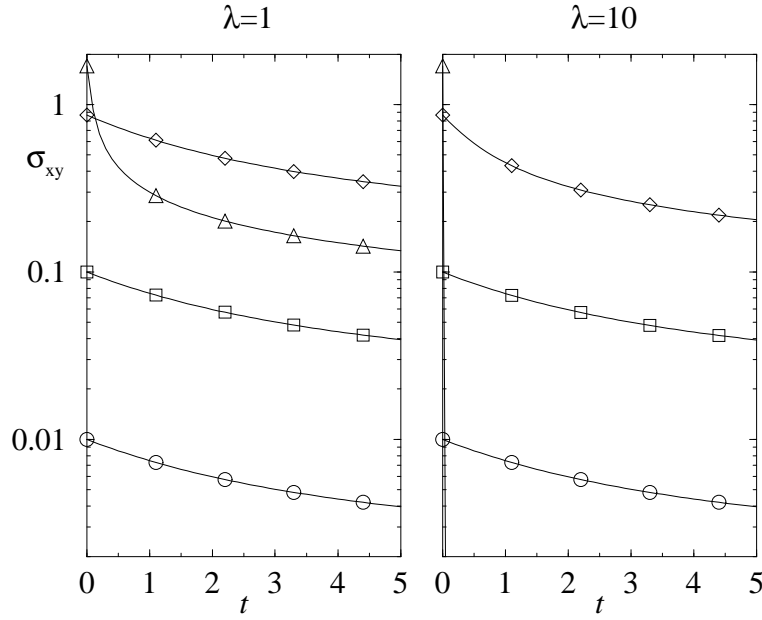


Figure 1: Stress relaxation after step shear strain, calculated within Model 2 at effective temperature $x = 1.5$. Strain amplitudes are $\gamma = 0.01$ (circles), 0.1 (squares), 1 (diamonds), 10 (triangles). The two plots show the effect of variation of the parameter λ : from Eqs.13 and 20, larger λ implies greater speed-up of the stress relaxation. For $\gamma = 10$ and $\lambda = 10$ (right), this speed-up is so large that the stress relaxes to zero essentially instantaneously on the scale of the plot. The nonlinear dependence of the initial value of the stress on γ , which arises from the factor $\mathbf{Q}(\mathbf{E})$ in Eq.20, is independent of λ and therefore the same in both plots.

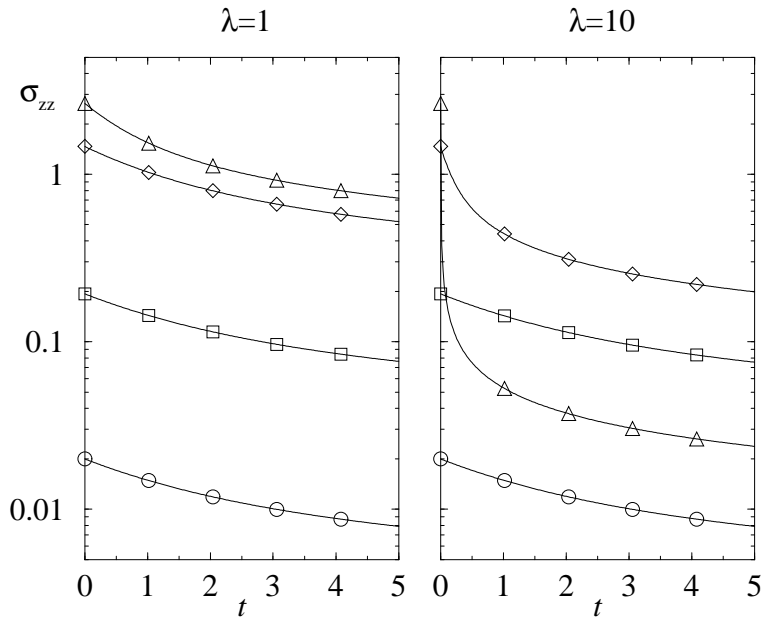


Figure 2: Analogue of figure 1 for step uniaxial extension. Shown is the relaxation of σ_{zz} , calculated within Model 2 at effective temperature $x = 1.5$. Strain amplitudes are $\epsilon = 0.01$ (circles), 0.1 (squares), 1 (diamonds), 2 (triangles). For the smaller ϵ , the initial stress response is linear, $\sigma_{zz} = 2\epsilon$, but at $\epsilon = 1$ and 2 the expected nonlinear deviations from this become apparent.

Next we consider steady shear flow, with shear rate $\dot{\gamma}$. From Eq.11 one finds that the stress tensor in the steady state is given by

$$\boldsymbol{\sigma} = \frac{\int_0^\infty d\gamma \mathbf{Q}(\gamma) G_1 \left(\dot{\gamma}^{-1} \int_0^\gamma d\gamma' e^{R(\gamma')/x} \right)}{\int_0^\infty d\gamma G_1 \left(\dot{\gamma}^{-1} \int_0^\gamma d\gamma' e^{R(\gamma')/x} \right)} \quad (25)$$

where $\mathbf{Q}(\gamma)$ and $R(\gamma')$ are \mathbf{Q} and R evaluated for a shear deformation with strain γ and γ' , respectively. As in the scalar SGR model, one deduces that for sufficiently large x the integrals over γ are dominated by values $\gamma \propto \dot{\gamma}/\Gamma_0 = \dot{\gamma}$ (recall that our underlying relaxation rate has been set to $\Gamma_0 = 1$). This then gives Newtonian behaviour at small shear rates, with $\sigma_{xy} \propto \dot{\gamma}$ and $N_1, N_2 \propto \dot{\gamma}^2$. As x approaches the glass transition at $x = 1$, however, values of $\gamma \gg \dot{\gamma}/\Gamma_0$ remain important for small $\dot{\gamma}$. These cause non-Newtonian singularities in the low- $\dot{\gamma}$ behaviour,

$$\sigma_{xy} \propto \begin{cases} \dot{\gamma}^{x-1} & \text{for } 1 < x < 2 \\ \text{const.} & \text{for } x < 1 \end{cases} \quad N_1, N_2 \propto \begin{cases} \dot{\gamma}^{x-1} & \text{for } 1 < x < 3 \\ \text{const.} & \text{for } x < 1 \end{cases} \quad (26)$$

These power laws, and the yield stress behaviour for $x < 1$, are largely independent of the particular forms of \mathbf{Q} and R . They only rely on $\sigma_{xy} \propto \gamma$ and $N_1, N_2 \propto \gamma^2$ for small γ , and on the growth of $R(\gamma)$ with γ eventually limiting the largest element strains that occur in the steady state. An interesting observation is that the non-Newtonian effects in the normal stress differences manifest themselves in a larger region above the glass transition (up to $x = 3$) than for the shear stress (up to $x = 2$). Another notable feature is that, when both are anomalous ($x \leq 2$), normal and shear stresses obey the *same* power law, in contrast to the familiar analytic case ($\sigma \sim \dot{\gamma}, N \sim \dot{\gamma}^2$). Figure 3 shows some example results, calculated from Model 2 with $\lambda = 1$. The crossover from yield stress behaviour for $x < 1$ to non-Newtonian power laws for $x > 1$ to Newtonian flow for $x > 2$ or $x > 3$ can clearly be seen. For larger λ , strain-induced yielding is more pronounced. This has two effects: it limits the element strains γ in steady state, so that at given $\dot{\gamma}$ both σ_{xy} and N_1 decrease with increasing λ . It also means that nonlinearities caused by strain-induced yielding are stronger, and deviations from the small- $\dot{\gamma}$ behaviour of Eq.26 therefore appear for smaller $\dot{\gamma}$. Numerical results for $\lambda = 10$ (not shown) confirm these expectations.

Finally, we consider a somewhat more complicated scenario, namely stress relaxation after cessation of a steady flow. From Eq.11 one finds for this case that the stress at a time t after cessation of the flow is

$$\boldsymbol{\sigma}(t) = \frac{\int_0^\infty d\gamma \mathbf{Q}(\gamma) G_1 \left(t + \frac{1}{\dot{\gamma}} \int_0^\gamma d\gamma' e^{R(\gamma')/x} \right)}{\int_0^\infty d\gamma G_1 \left(\frac{1}{\dot{\gamma}} \int_0^\gamma d\gamma' e^{R(\gamma')/x} \right)} \quad (27)$$

For $t = 0$, this just gives the steady state shear of Eq.25. Eqs.25,27 generalize straightforwardly to other steady flows (and their cessation); e.g. for an extensional flow one merely replaces γ and $\dot{\gamma}$ by ϵ and $\dot{\epsilon}$ everywhere.

We now give a brief scaling analysis of the behaviour predicted by Eq.27, focussing on the regime where all timescales ($\dot{\gamma}^{-1}$ and t) are large compared to the microscopic timescale Γ_0^{-1} , which equals unity in our chosen units. The reasoning

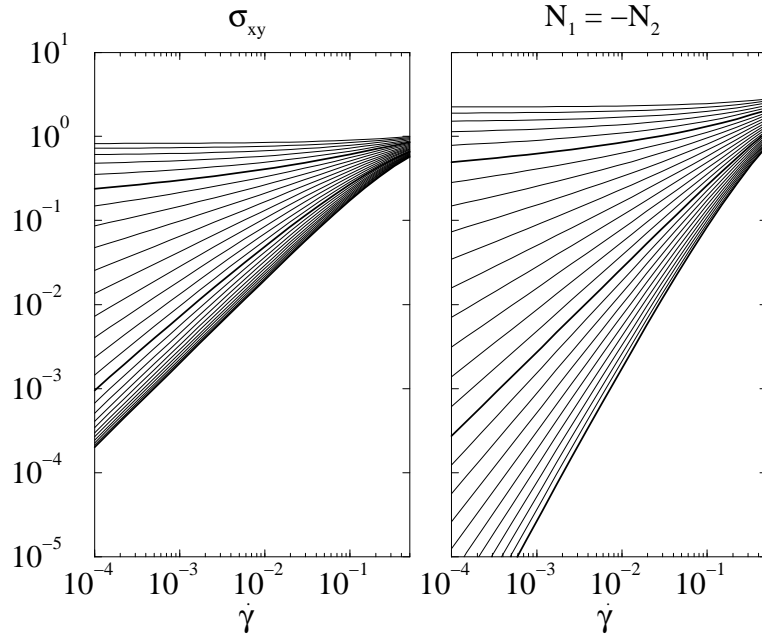


Figure 3: Results for steady shear, showing shear stress σ_{xy} (left) and normal stress differences (right) as a function of shear rate $\dot{\gamma}$, as calculated within Model 2 with $\lambda = 1$. The curves from top to bottom are for a series of increasing noise temperatures $x = 0.5, 0.6, \dots, 3$, with $x = 1$ and $x = 2$ highlighted in bold. Note that, for small $\dot{\gamma}$, the shear stress shows Newtonian behaviour $\sigma_{xy} \propto \dot{\gamma}$ for $x > 2$, while for the normal stress differences non-Newtonian behaviour persists up to $x = 3$. For $x < 1$ the curves tend to nonzero limits for $\dot{\gamma} \rightarrow 0$, demonstrating that the system exhibits a (dynamic) yield stress.

is similar to that used for other rheological predictions of the (scalar) SGR model (Sollich, 1998; Fielding et al., 2000). One uses the following facts. The function G_1 has the initial value $G_1(0) = 1$; for $z \gg 1$ it decays as $G_1(z) \sim t^{-x}$. The integral $\int_0^\gamma d\gamma' e^{R(\gamma')/x}$ is $\approx \gamma$ for small γ but eventually grows very quickly with γ , in fact typically exponentially since $R(\gamma')$ grows at least as a power of γ' . In the denominator of Eq.27, one can thus limit the γ -integration to the $O(1)$ range before this exponential cutoff sets in. Separating the regimes where $\gamma \leq O(\dot{\gamma})$ (and thus the argument of G_1 is $O(1)$) and $\gamma \geq O(\dot{\gamma})$ (where the asymptotic power law decay of G_1 is a good approximation), one finds that the denominator scales as $\dot{\gamma}$ for $x > 1$ and as $\dot{\gamma}^x$ for $x < 1$. In the numerator of Eq.27 one can use a similar analysis, though the small- γ regime does not need to be treated separately since for $t \gg 1$ the argument of G_1 is always large. For $\dot{\gamma}t \ll 1$, the integral can again be cut off at $\gamma = O(1)$; depending on the value of x , it can be dominated by the regime of small $\gamma = O(\dot{\gamma})$ and one then needs to bear in mind that generically $Q_{xy}(\gamma) \sim \gamma$ while normal stress differences such as $Q_{xx}(\gamma) - Q_{yy}(\gamma)$ scale as γ^2 for small γ . For $\dot{\gamma}t \gg 1$, on the other hand, the cutoff in γ is located where $\dot{\gamma}t \approx \int_0^\gamma d\gamma' e^{R(\gamma')/x}$ and so typically grows logarithmically with $\dot{\gamma}t$; in the latter case strains γ of $O(1)$ – up to the cutoff – always dominate the integral. Putting these elements together, one finds for the relaxation of the shear stress

$$\frac{\sigma_{xy}(t)}{\sigma_{xy}(0)} \simeq \begin{cases} 1 & \text{for } t \ll \dot{\gamma}^{-1} \\ (\dot{\gamma}t)^{-x} & \text{for } t \gg \dot{\gamma}^{-1} \end{cases} \quad \text{for } x < 2$$

$$\begin{cases} t^{2-x} & \text{for } t \ll \dot{\gamma}^{-1} \\ t^{2-x}(\dot{\gamma}t)^{-2} & \text{for } t \gg \dot{\gamma}^{-1} \end{cases} \quad \text{for } x > 2 \quad (28)$$

and for a typical normal stress difference such as N_1

$$\frac{N_1(t)}{N_1(0)} \simeq \begin{cases} 1 & \text{for } t \ll \dot{\gamma}^{-1} \\ (\dot{\gamma}t)^{-x} & \text{for } t \gg \dot{\gamma}^{-1} \end{cases} \quad \text{for } x < 3$$

$$\begin{cases} t^{3-x} & \text{for } t \ll \dot{\gamma}^{-1} \\ t^{3-x}(\dot{\gamma}t)^{-3} & \text{for } t \gg \dot{\gamma}^{-1} \end{cases} \quad \text{for } x > 3 \quad (29)$$

In Eqs.28,29 the power laws for $t \gg \dot{\gamma}^{-1}$ are all subject to logarithmic corrections in $\dot{\gamma}t$, which arise from the variation of the γ -cutoff discussed above. The scalings given apply to the generic tensorial SGR model of Eq.11, including in particular our Models 1–3. The glassy nature of the model is manifested in the relaxations scaling with $\dot{\gamma}t$ for low enough x , rather than with t as one would expect if the microscopic timescale dominates the dynamics. As in the results for steady shear, Eq.26, glassy effects remain important up to higher x for normal stress differences ($x = 3$) than for the shear stress ($x = 2$).

In figure 4 we show some numerical results, calculated from Eq.27 within Model 1 with $\lambda = 1$. The power laws predicted by Eqs.28,29 are quite well obeyed, subject to the expected logarithmic corrections for $t \gg \dot{\gamma}^{-1}$. As a general trend, we note that the normal stress difference N_1 decays more slowly than the shear stress σ_{xy} . This is certainly true for $x > 3$, where N_1 decays with a slower power law than σ_{xy} from Eqs.28,29, and for $2 < x < 3$ where N_1 remains essentially constant for $t \ll \dot{\gamma}^{-1}$. From figure 4 we also observe the same trend for $x < 2$,

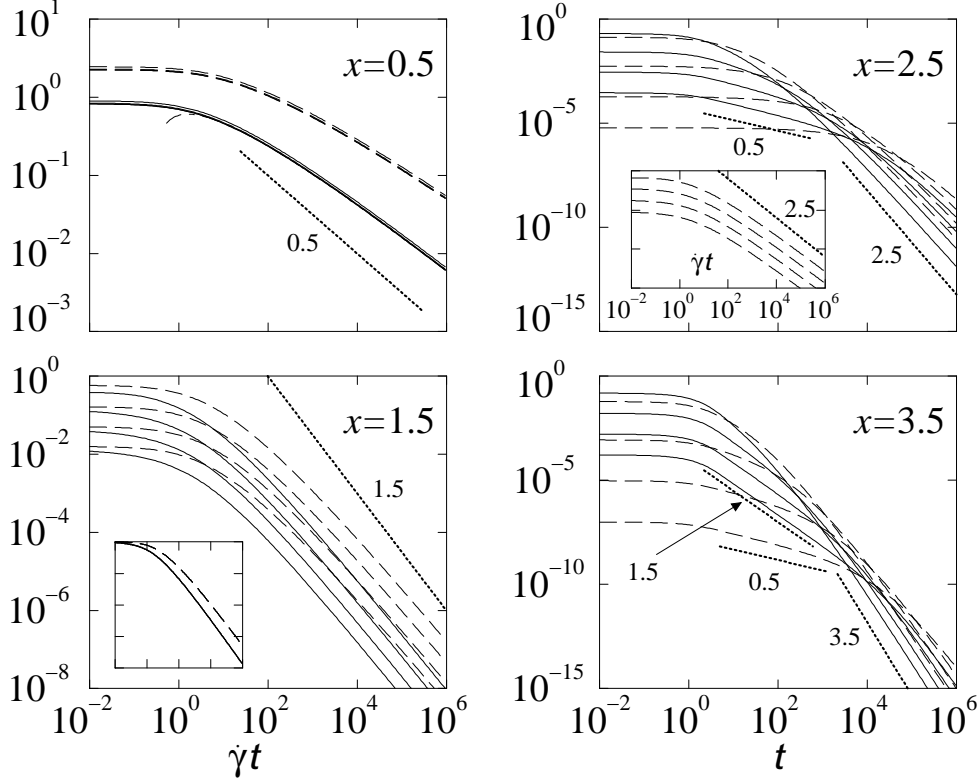


Figure 4: Results for cessation of steady shear flow, calculated within Model 2 with $\lambda = 1$, for four different noise temperatures x . Shear stress σ_{xy} and first normal stress difference $N_1 = -N_2$ are plotted as solid and dashed lines, respectively; in each graph a set of four curves are shown for each quantity, for shear rates $\dot{\gamma} = 10^{-4}, 10^{-3}, 10^{-2}, 10^{-1}$ from bottom to top. Theoretically predicted power laws from Eqs.28,29 are shown by bold dotted lines and annotated with their (negative) slopes. Top left: For $x = 0.5$; both σ_{xy} and N_1 scale with $\dot{\gamma}t$. Logarithmic corrections to the predicted decay $\sim (\dot{\gamma}t)^{-x}$ are non-negligible in the range of $\dot{\gamma}t$ shown. The underlying power law is nevertheless correct, as a fit of $\sigma_{xy}(t)$ for $\dot{\gamma} = 10^{-4}$ to the form $[a \ln(\dot{\gamma}t) + b](\dot{\gamma}t)^{-1/2}$ shows (dashed-dotted line, just distinguishable around $\dot{\gamma}t = 1$). Bottom left: $x = 1.5$; the larger decay exponent $(\dot{\gamma}t)^{-x}$ now makes logarithmic corrections less important. In the inset the curves are rescaled vertically by their value at $t = 0$ to show that their time dependence is otherwise identical. Top right: $x = 2.5$. The shear stress σ_{xy} follows the predicted power laws from Eq.28 quite well. In contrast to σ_{xy} , the normal stress difference only decays significantly for $t \gg \dot{\gamma}^{-1}$, scaling throughout with $\dot{\gamma}t$. This is shown in the inset where (on the same vertical scale) N_1 is plotted against $\dot{\gamma}t$. Bottom right: for $x = 3.5$, both σ_{xy} and N_1 decay for $t \ll \dot{\gamma}^{-1}$.

however: even though Eqs.28,29 predict that σ_{xy} and N_1 should have the same asymptotic decay shapes in this regime, N_1 is seen to decay more slowly than σ_{xy} , presumably due to stronger logarithmic corrections.

4 Conclusions

In this work we have presented a general strategy for alleviating one of the more serious restrictions of the SGR model for soft glasses, namely its effectively scalar treatment of stress and strain, which results in an inability to consider normal stresses or flows other than simple shear. As might be expected, the tensorialization allows significant scope for tailoring the model to different classes of soft material, without altering the rather simple basic assumptions that underlie it. In particular, we have presented results for several tensorial SGR variants that offer a possible description of flowing foams and/or dense emulsions. Because of the amorphous packings and slow dynamics observed in these materials, they are prime candidates for the physical picture that underlies the SGR model. It is useful, we believe, to have a constitutive equation that can capture to reasonable accuracy the step-strain response of real foams (Model 3 is probably best in this respect) while also predicting nontrivial yield behavior, flow curves, and aging phenomena. These three features all arise in the glass phase of the model ($x \leq 1$) which is therefore the one most likely to be of interest in foam flows, except perhaps very close to the onset of rigidity which occurs at volume fractions of the dispersed phase of around 58% (Mason et al., 1996).

As emphasized elsewhere (Sollich et al., 1997; Sollich, 1998; Fielding et al., 2000), the absence of tensorial structure is by no means the only shortcoming of the scalar SGR model; its various assumptions are all questionable at several levels and, even after tensorialization, the approach should not be viewed as complete in any sense. Experimental falsifications of its predictions are welcome, since these will help direct theoretical work towards more complete models. (Verifications are, of course, also welcome.) Our development in this paper of tensorial versions of SGR should certainly allow more stringent comparisons to be drawn between theory and experiments.

Indeed, in rheological terms one could argue that a proper tensorial treatment of stress and strain is the absolute minimum required for any kind of serious predictive modelling to begin. In this sense, the models presented in this paper could represent a ‘coming of age’ for the SGR approach to the rheology and rheological aging of soft materials. Despite the shortcomings of SGR, we are not aware of any competing approaches that directly confront the nonergodic features of these systems within a rheological context.

Acknowledgements

We acknowledge useful discussions with M Doi, A Kraynick, R Höhler, and C Holmes. We thank the Newton Institute, where part of this work was done, for hospitality.

References

- J P Bouchaud. Weak ergodicity breaking and aging in disordered-systems. *J. Phys. (France) I* **2**, 1705–1713 (1992).
- J P Bouchaud, A Comtet, and C Monthus. On a dynamical model of glasses. *J. Phys. (France) I* **5**, 1521–1526 (1995).
- M E Cates. Structural relaxation and rheology of soft condensed matter. In J L Barrat and J Kurchan, editors, *Slow Relaxations and Nonequilibrium Dynamics in Condensed Matter (77th Les Houches Summer School)*. Springer, 2003.
- M Cloître, R Borrega, and L Leibler. Rheological aging and rejuvenation in microgel pastes. *Phys. Rev. Lett.* **85**, 4819–4822 (2000).
- M Cloître, R Borrega, F Monti, and L Leibler. Glassy dynamics and flow properties of soft colloidal pastes. *Phys. Rev. Lett.* **90** 068303 (2003).
- S Cohen-Addad and R Höhler. Bubble dynamics relaxation in aqueous foam probed by multispeckle diffusing-wave spectroscopy. *Phys. Rev. Lett.* **86**, 4700–4703 (2001).
- M Doi and T Ohta. Dynamics and rheology of complex interfaces. 1. *J. Chem. Phys.* **95**, 1242–1248 (1991).
- S M Fielding, P Sollich, and M E Cates. Aging and rheology in soft materials. *J. Rheol.* **44**, 323–369 (2000).
- D A Head, A Ajdari, and M E Cates. Jamming, hysteresis, and oscillation in scalar models for shear thickening. *Phys. Rev. E* **64**, 061509 (2001).
- D A Head, A Ajdari, and M E Cates. Rheological instability in a simple shear-thickening model. *Europhys. Lett.*, **57**, 120–126 (2002).
- R Höhler, S Cohen-Addad, and A Asnacios. Rheological memory effect in aqueous foam. *Europhys. Lett.* **48**, 93–98 (1999).
- S D Holdsworth. Rheological models used for the prediction of the flow properties of food products. *Trans. Inst. Chem. Eng.* **71**, 139–179 (1993).
- R G Larson. The elastic stress in “film fluids”. *J. Rheol.* **41**, 365–372 (1997).
- T G Mason, J Bibette, and D A Weitz. Yielding and flow of monodisperse emulsions. *J. Coll. Interf. Sci.* **179**, 439–448 (1996).
- E Michel, J Appell, F Molino, J Kieffer, and G Porte. Unstable flow and non-monotonic flow curves of transient networks. *J. Rheol.* **45**, 1465–1477 (2001).
- D A Reinelt and A M Kraynik. Simple shearing flow of dry soap foams with tetrahedrally close-packed structure. *J. Rheol.* **44**, 453–471 (2000).
- P Sollich. Rheological constitutive equation for a model of soft glassy materials. *Phys. Rev. E* **58**, 738–759 (1998).

- P Sollich, F Lequeux, P Hébraud, and M E Cates. Rheology of soft glassy materials. *Phys. Rev. Lett.* **78**, 2020–2023 (1997).
- V Viasnoff, S Jurine, and F Lequeux. How colloidal suspensions that age are rejuvenated by strain application. *Faraday Discussions* **123**, 253–266 (2003).
- V Viasnoff and F Lequeux. Rejuvenation and overaging in a colloidal glass under shear. *Phys. Rev. Lett.* **89**, 065701 (2002).